Solvent-Controlled Electron Transfer in Crystal Violet Lactone

ARTICLE *in* THE JOURNAL OF PHYSICAL CHEMISTRY A · APRIL 2011

Impact Factor: 2.69 · DOI: 10.1021/jp106240x · Source: PubMed

THE JOURNAL OF PHYSICAL CHEMISTRY A

ARTICLE

pubs.acs.org/JPCA

Solvent-Controlled Electron Transfer in Crystal Violet Lactone

Xiang Li and Mark Maroncelli*

The Pennsylvania State University, University Park, Pennsylvania 16802, United States

ABSTRACT: Steady-state and picosecond time-resolved emission experiments are used to examine the excited-state charge transfer reaction of crystal violet lactone (CVL) in aprotic solvents. Solvatochromic analysis using a dielectric continuum model suggests dipole moments of 9−12 D for the initially excited (LE) state and ∼24 D for the charge-transfer (CT) state. Intensities of steady-state emission as well as kinetic data provide free energies for the LE → CT reaction that range from +12 kJ/mol in nonpolar solvents to −10 kJ/mol in highly polar solvents at 25 °C. Reaction rates constants, which lie in the range of 10−100 ns^{-1} in most solvents, depend on both solvent polarity and solvent friction. In highly polar solvents, rates are correlated to solvation times in a manner that indicates that the reaction is a solvent-controlled electron transfer on an adiabatic potential surface having a modest barrier.

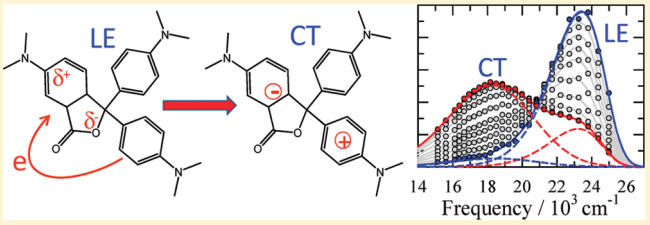

1. INTRODUCTION

Crystal violet lactone (CVL; Figure 1) exhibits dual emission in fluid solution[1,2] as a result of a rapid excited-state charge transfer reaction.[3] Although several groups have begun to use this solute to probe various aspects of solvent-reactant coupling in ionic liquids,[4−8] the solvent dependence of the CVL reaction in conventional solvents is not yet fully characterized. The present Article describes photophysical measurements of CVL in a variety of conventional polar aprotic solvents intended to provide a more complete description of the reaction in conventional solvents, in particular, how the driving force and rate of the charge transfer depend on solvent properties.

Although the photophysics of CVL had been previously studied in the context of color formation and polymerization,[9,1] it was only recently that Karpiuk first explored the excited-state reaction giving rise to the dual fluorescence of CVL.[3] Using model compounds resembling the structural components of CVL,[10,11] Karpiuk demonstrated that excitation of the lowest-energy electronic absorption leads to a polar excited state localized on the dimethylaminophthalide chromophore.[3] Solvatochromic analysis lead to an estimate of ∼11 D for the dipole moment of this "locally excited" state (denoted "LE" here and "CT_A" by Karpiuk). He also showed that the second emission band, which is observed to the red of the LE band in polar solvents, is due to the transfer of an electron from one of the dimethylaminobenzonitrile moieties to the aminophthalide subsystem (Figure 1). The dipole moment of this charge transfer state ("CT" here; "CT_B" in Karpiuk's notation) was estimated to be ∼25 D.[3] Later transient absorption measurements in three polar aprotic solvents by Schmidhammer et al.[12] indicated that equilibrium between the LE and CT states is established on the 10 ps time scale. Because these times are roughly comparable to solvation times, they proposed that the charge transfer reaction is controlled by the solvent's dynamics.[12]

Karpiuk also observed that the behavior of CVL in alcohol solvents differs markedly from that in aprotic solvents. In alcohols, only the LE band is observed. In addition, the emission lifetime and quantum yield (φ) are much smaller in alcohols compared with aprotic solvents of like polarity. For example, $\varphi = 5 \times 10^{-4}$ in methanol compared with 4×10^{-3} in acetonitrile.[3] The similarity of the nanosecond transient absorption spectra of CVL in 1-propanol to that of crystal violet lead Karpiuk to conclude that rapid C−O bond cleavage occurs in alcohols and potentially in other solvents capable of hydrogen bond donation. Very recently Santhosh and Samanta[6] noted that CVL has reduced lifetimes in 1,3-dialkylimidazolium ionic liquids, suggesting that such reaction might occur even in these weakly protic solvents.

The present work represents an extension of the characterization studies already reported by Karpiuk and coworkers on CVL and related molecules.[2,10,3,11,13,12] We focus here on conventional polar aprotic solvents to avoid complications of the lactone ring-opening noted above. We use steady-state and picosecond time-resolved emission spectroscopy to establish more definitively the effects of solvent polarity and solvation dynamics on the LE → CT reaction of CVL. We find that the emission spectra and kinetics of CVL bear many resemblances to those of the "PnC" series of alkylaminobenzonitriles we have previously studied.[14] Our paper on this earlier work therefore provides a useful reference for more detailed discussions of the models and analysis methods used here. As in the case of the PnC molecules, the excited-state reaction is sufficiently rapid relative to the lifetime of the excited state that the relative LE and CT band

Special Issue: Graham R. Fleming Festschrift

Received: July 6, 2010
Revised: August 22, 2010
Published: September 10, 2010

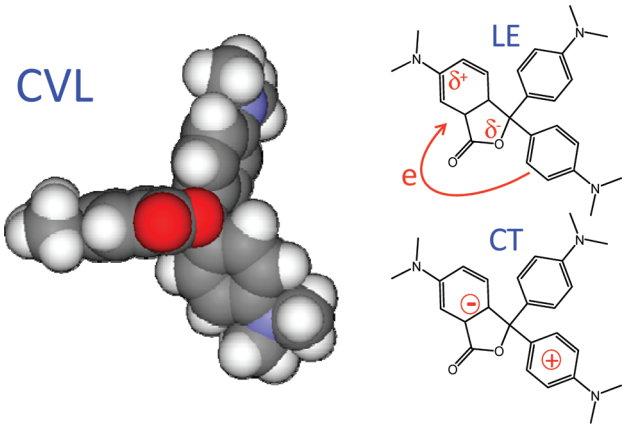

Figure 1. Space-filling model of CVL and schematic illustration of the LE and CT excited states and the electron transfer reaction connecting them. The space-filling model shows the optimized ground-state geometry calculated from a CAM-B3LYP/6-311G(d) calculation.

intensities in the steady-state spectrum reflect the equilibrium populations of these two states. We therefore first survey the steady-state spectra observed in a range of nonpolar and polar aprotic solvents to help establish the energetics of reaction. We then describe time-resolved emission experiments used to measure reaction rates and discuss how these rates are correlated to both solvent polarity and dynamical solvent properties.

2. EXPERIMENTAL SECTION

CVL was obtained from Sigma-Aldrich (97%) and crystallized twice from acetone prior to use. After recrystallization, no fluorescent impurities could be detected by any observable excitation dependence of its emission spectrum in low viscosity solvents. The solvents used here were spectroscopic or HPLC grade (typically >99%) obtained from Sigma-Aldrich. Samples for steady-state spectroscopy were prepared in 1 cm quartz cuvettes at concentrations providing optical densities of <0.2 at the excitation wavelength. Absorption measurements were made using a Hitachi U-3000 UV/visible spectrophotometer with a resolution of 1 nm. Corrected emission spectra were recorded with a PTI spectrometer at 2 nm resolution. Solvent blanks were subtracted from all spectra, and the spectra were converted to a frequency representation prior to analysis.

Time-resolved emission decays were collected using a time-correlated single-photon counting instrument based on a femtosecond Ti/sapphire laser. Samples were contained in 1 cm cuvettes into which a yellow filter glass was inserted to remove reflections near time zero. Selected filters were also used in the emission path to remove stray excitation light. Emission was collected at magic angle through an ISA H10 monochromator using an emission band-pass of 8 nm. Data were collected with a resolution of 0.8 ps/channel for capturing the reaction kinetics and lower resolutions for better determining long decay components present in less polar solvents. The response time of the instrument was 25 ps (fwhm), as measured using a scattering solution. Emission transients were fit using an iterative reconvolution algorithm that enables reliable measurement of decay components as fast as 5 ps. In most solvents, three or four pairs of decays at selected wavelengths were collected and averaged to determine reaction times and equilibrium constants. In several solvents, decays at 10−20 wavelengths spanning the emission

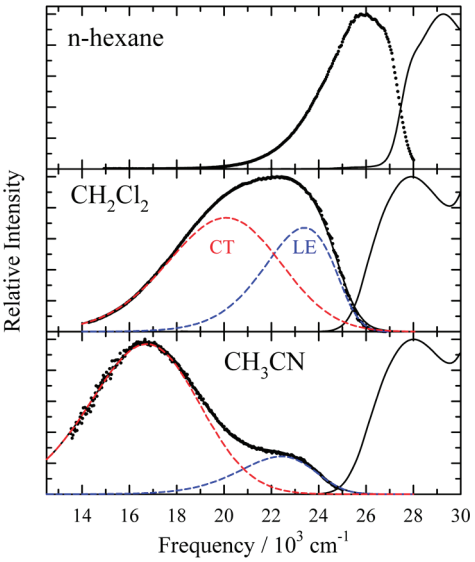

Figure 2. Representative absorption and emission spectra of CVL in *n*-hexane, dichloromethane, and acetonitrile. Observed emission spectra are shown as points. Fits (solid curves) and their decompositions into LE and CT contributions are shown as dashed curves.

spectrum were collected to produce more complete time-resolved spectra via spectral reconstruction.[15] Unless otherwise stated, both steady-state and time-resolved samples were maintained at 25.0 ± 0.2 °C using a circulating water bath. Samples were deoxygenated by bubbling with dry nitrogen gas for 15 min prior to data collection. Variable temperature data at temperatures lower than 10 °C were collected using an Oxford DN-1400 liquid nitrogen cryostat.

3. RESULTS AND DISCUSSION

A. Steady-State Spectra. Representative spectra of CVL in three solvents are shown in Figure 2. In nonpolar solvents such as *n*-hexane, a single emission band is observed. This band bears a mirror image relationship to the lowest energy absorption band, and it appears to originate from the same excited electronic state. As already mentioned, based on the similar S_1 absorption and emission bands of 6-dimethylaminophthalide, Karpiuk[3] assigned this transition to an excited state "LE" primarily localized on the aminophthalide ring of CVL. In solvents having relative permittivities $\varepsilon \geq 4$, a second emission band at lower energies becomes evident. Similarity to the emission of malachite green lactone lead Karpiuk to assign this second band to emission from a charge transfer (CT) state reached by partial electron donation from one or both dimethylaniline portions of the molecule to the aminophthalide ring.[3] We note that the emission spectra shown in Figure 2 differ somewhat from those reported by Karpiuk (figure 3 of ref 3). Whereas peak frequencies are nearly the same, the shapes of broad bands such as the emission in CH_2Cl_2 and the relative LE/CT intensity ratios in solvents like CH_3CN shown in Figure 1 appear to differ significantly. Ref 3 does not state whether any correction was made for the wavelength-dependent responsivity of the spectrometer, and it is likely that differences in spectral correction are the source of this discrepancy.[16]

To quantify the solvent dependence of the frequencies and relative intensities of the emission bands, we employed fits based on a simple inhomogeneous broadening model.[17] Specifically, we

Table 1. Characteristics of Steady-State Spectra (25 °C)[a]

no.	solvent	ε	n_D	ν_{abs}	ν_{LE}	ν_{CT}	$\Delta\nu_{LE}$	$\Delta\nu_{CT}$	f_{CT}
1	*n*-hexane	1.88	1.372	29.27	25.87		0		
2	cyclohexane	2.02	1.424	29.15	25.79		0.07		
3	1,1,2-trichlorotrifluoroethane	2.41	1.356	28.96	25.22		0.79		
4	di-*n*-butyl ether	3.08	1.397	28.88	25.32		0.69		
5	di-isopropyl ether	3.88	1.366	28.92	25.22		0.85		
6	chloroform	4.89	1.442	27.98	23.21		2.29	2.76	0.77 ± 0.30
7	butyl acetate	5.01	1.392	28.56	24.30		1.47	2.48	0.34 ± 0.11
8	ethyl acetate	6.02	1.370	28.51	23.91		1.81	4.08	0.32 ± 0.12
9	methyl acetate	6.68	1.359	28.43	23.77		2.00	5.28	0.34 ± 0.05
10	1-chlorobutane	7.39	1.400	28.48	24.57		1.39	2.76	0.17 ± 0.08
11	tetrahydrofuran	7.58	1.405	28.47	24.01		1.68	4.25	0.30 ± 0.10
12	dichloromethane	8.93	1.421	27.77	(22.3)		2.46	5.45	0.64 ± 0.05
13	acetone	20.56	1.356	28.21	(23.0)	18.21	2.74	7.64	0.81 ± 0.05
14	butyronitrile	24.83	1.382	28.09	(23.5)	18.18	2.64	7.47	0.81 ± 0.05
15	acetonitrile	35.94	1.382	28.02	(23.2)	16.78	3.01	8.63	0.93 ± 0.05
16	*N*,*N*-dimethylformamide	36.71	1.428	27.90	(23.5)	17.32	2.97	8.27	0.89 ± 0.05
17	dimethylsulfoxide	46.45	1.477	27.70	(22.8)	16.64	3.40	9.08	0.85 ± 0.05
18	propylene carbonate	64.92	1.419	27.73	(23.2)	16.77	2.94	8.77	0.81 ± 0.05

[a] ε and n_D are the relative permittivity and refractive index of the solvent from ref 23. ν_{abs}, ν_{LE}, and ν_{CT} are peak frequencies of the S_1 absorption band and of the peaks of the high-frequencey (LE) and low-frequency (CT) bands measured directly from the emission spectra. Values in parentheses indicate estimates in cases where no true second maximum is present. $\Delta\nu_{LE}$ and $\Delta\nu_{CT}$ are the shifts of the LE and CT bands relative to *n*-hexane, and f_{CT} is the fractional area of the CT emission band based on the fitting method described in the text. In these fits, the inhomogeneous broadening of the CT band was fixed at 4300 cm^{-1}, and that of the LE band was assumed to depend on solvent according to $\Gamma_{LE}/cm^{-1} = 336 + 2080 d_{0.25}(\varepsilon,n_D^2)$. The latter parameters were chosen on the basis of unconstrained fits to the spectra and applied to help minimize variations in f_{CT} due the underdetermined nature of some fits. All frequencies are in units of 10^3 cm^{-1}.

assume that both bands can be represented by shifting and broadening an "unsolvated" vibronic line shape function using a Gaussian function to represent the distribution of solvent-induced frequency shifts present in a given solvent. For the line shape function of both bands, we use $L(\nu) \propto F_{np}(\nu)/\nu^3$ where $F_{np}(\nu)$ is the (LE) fluorescence spectrum observed in *n*-hexane. This approach does not provide absolute measures of the solvent shift or broadening of the CT emission, but it is nevertheless a useful and consistent way to dissect the spectra and determine relative information, especially the relative band intensities of most interest here. Two such fits are illustrated by the dashed curves in Figure 1. Characteristics of the steady-state emission spectra obtained from such fits along with peak frequencies of the S_1 absorption and emission peaks are summarized in Table 1.

To correlate these data with solvent properties, we use the spherical-polarizable-dipole solute, dielectric continuum solvent model described in refs 14 and 18. Transition frequencies (*tr* = abs or em) are assumed to depend on solvent dielectric properties according to

$$h\nu_{tr} = h\nu_{tr}^0 + A_{tr} d_c(n^2) + C_{tr}\{d_c(\varepsilon) - d_c(n^2)\} \quad (1a)$$

$$A_{tr} = -(\mu_f^2 - \mu_i^2)a^{-3}C_{tr} = -2\vec{\mu_i}\cdot(\vec{\mu_f} - \vec{\mu_i})a^{-3} \quad (1b)$$

where $h\nu_{tr}^0$ is the transition energy in the gas phase. Solute parameters in this description are the dipole moments in the initial, i, and final, f, electronic states of the transition, and the cavity size, *a*, and polarizability, α, are both assumed independent of state. d_c is a reaction field factor

$$d_c(x) \equiv \frac{d_0(x)}{1 - 2c d_0(x)} \quad d_0(x) \equiv \frac{x-1}{2x+1} \quad (2)$$

which depends on solute polarizability via the ratio $c = \alpha/a^3$. Here we assume $c = 0.25$, a value intermediate between the non-polarizable ($c = 0$) and Clausius−Mossotti ($c = 1/2$) limits. The particular value used is of little consequence for the present purposes.

Figure 3 shows that the solvatochromic shifts of the S_1 absorption (peak) and the LE and CT bands of CVL are reasonably represented by this model. The coefficients A_{tr} and C_{tr}, obtained from bilinear fits to the data in Table 1 combined with data from mixtures of methyl acetate + acetone (green squares in Figure 3) and acetonitrile + propylene carbonate (green triangles), are compiled in Table 2. In principle, these fit parameters can be used to calculate changes in the dipole moments associated with the various transitions, and Karpiuk discusses such calculations in some detail.[3] In the case of CVL, there is a great deal of ambiguity in using the model described above (or any other simple model) to deduce dipole moments due to the highly nonspherical shape of this molecule (Figure 1). On the basis of comparisons to the component chromophores of CVL, Karpiuk proposed the use of two different effective spherical radii, $a = 3.6$ Å for analyzing the LE emission (and $S_0 \rightarrow$ LE absorption) and $a = 5.8$ Å for the CT emission. Adopting these same choices for cavity radii and a ground-state dipole moment of 6.0 D from B3LYP/6-311G(d) calculations,[19] the results in Table 2 suggest a dipole moment of 9−12 D in the LE state and about 24 D in the CT state. Although we have little confidence in the accuracy of these estimates, they are close to the values obtained by Karpiuk, based on a different solvatochromic approach. We also note that a dipole moment of 24 D for the CT state is equivalent to separation of $\pm 1e$ over a distance of 5 Å. The distance between the centers of mass of the donor

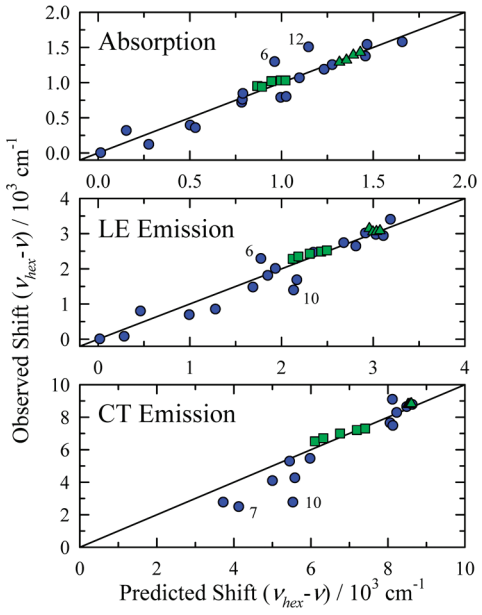

Figure 3. Correlation of spectral shifts measured relative to frequencies in *n*-hexane with solvent dielectric properties. The blue points are data in the pure solvents listed in Table 1, the green squares are from mixtures of acetone + methyl acetate, and green triangles are from propylene carbonate + acetonitrile mixtures. Numbers indicate specific solvents, as listed in Table 1.

Table 2. Summary of Solvatochromic Fits[a]

	Abs ν_{pk}	Em ($\nu_{hex} - \nu_{LE}$)	Em ($\nu_{hex} - \nu_{CT}$)
$h\nu^0_{tr}$	31.71 ± 0.43	−2.49 ± 0.86	−3.1 ± 2.8
A_{tr}	−12.2 ± 2.0	12.3 ± 4.1	8.9 ± 12
C_{tr}	−2.87 ± 0.21	6.73 ± 0.42	23.2 ± 2.1
N_{obs}	27	27	23
R	0.95	0.96	0.93
σ_{fit}	0.14	0.28	0.81

[a] $h\nu^0_{tr}$, A_{tr}, and C_{tr} are the coefficients in eqs 1a, 1b, and 2 in units of 10^3 cm^{-1}. The column "Abs ν_{pk}" lists coefficients of the fits to absorption peak frequencies and the columns "Em ($\nu_{hex} - \nu_{tr}$)" are those of fits of the emission shifts relative to *n*-hexane. N_{obs}, R, and σ_{fit} denote the number of data points, the linear correlation coefficient, and the standard error of each fit.

dimethylaniline and aminophthalide rings is 5.6 Å, consistent with virtually complete electron transfer in the CT state.

Figure 4 illustrates the changes in emission observed as a function of temperature in the solvent *n*-butyronitrile. Over the temperature range shown, both the LE and CT bands shift to higher frequencies with increasing temperature as a result of the decreasing density and polarity of the solvent. These approximately linear shifts are characterized by temperature derivatives of 5.4 (LE) and 11 cm^{-1} K^{-1} (CT). Of most interest in Figure 4 is the nonmonotonic variation of the relative intensities of the LE and CT bands. These intensities are shown in the form of a "Stevens−Ban plot"[20] in Figure 5. Also included are analogous data in propylene carbonate. If certain requirements are met, then the high-temperature limiting slopes in such plots provide estimates of the reaction enthalpy, Δ_rH, and the low-temperature slope provides estimates of the activation enthalpy, Δ_rH^*, of the LE → CT reaction.[20−22] The data in Figure 5 provide $\Delta_rH = -17 \pm 1$ kJ/mol and $\Delta_rH^* = 11 \pm 2$ kJ/mol in butyronitrile and

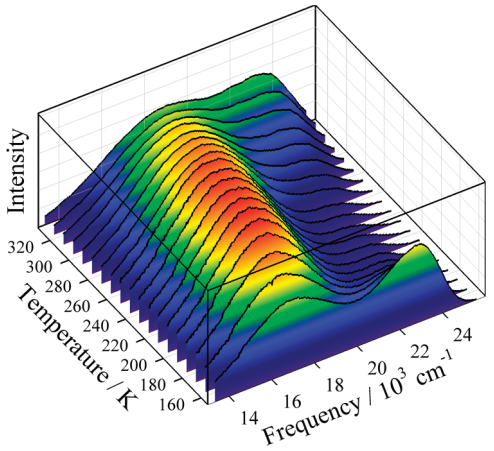

Figure 4. Temperature dependence of the steady-state emission of CVL in *n*-butyronitrile. Spectra have been area-normalized to display the relative intensity changes of the LE and CT bands.

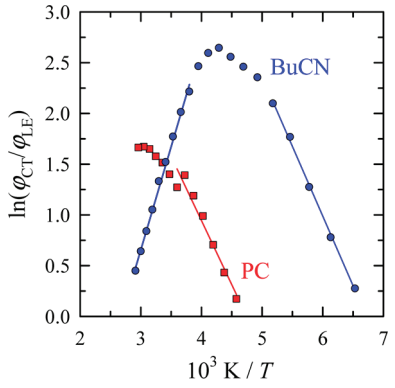

Figure 5. "Stevens−Ban" plots of the ratio of integrated intensities of the CT and LE emission bands of CVL in *n*-butyronitrile (BuCN) and propylene carbonate (PC). The lines shown here are fits to the limiting low- and high-temperature slopes that provide estimate of Δ_rH^* and Δ_rH, respectively.

$\Delta_rH^* = 12 \pm 3$ kJ/mol in propylene carbonate. Although we do not expect the activation enthalpies determined in this way to be as accurate as those deduced from the time-resolved data discussed below, we note that these values of Δ_rH^* are close to the viscosity activation energies of the two solvents, E_η = 8.7 kJ/mol in butyronitrile and 16 kJ/mol in propylene carbonate (at 25 °C).[23]

B. Time-Resolved Emission and Kinetic Model. Representative time-resolved emission decays of CVL in acetone are shown in Figure 6. These decays are typical of what is observed in moderate- to high-polarity solvents. Emission near the peak of the LE maximum undergoes a pronounced rapid decay with a time constant in the 10−30 ps range, followed by a small amplitude component having a nanosecond time constant. In the region of the CT emission, there is a fast rise and slow decay with essentially the same two time constants. Multiexponential fits are illustrated by the weighted residuals at the top of Figure 6, and the parameters obtained from these fits are shown in the inset table. In many cases, a purely biexponential function does not fit the transients in the LE region to within statistical uncertainties. A third, small amplitude (2% here) component with an intermediate time constant is often necessary. We believe

dx.doi.org/10.1021/jp106240x |*J. Phys. Chem. A* 2011, 115, 3746–3754

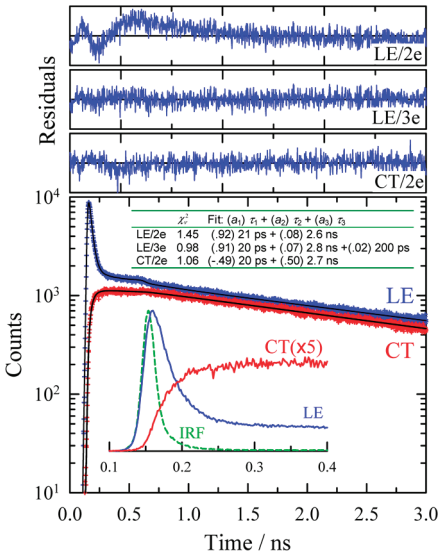

Figure 6. Representative emission decays of CVL in acetone (25 °C). The points on the bottom are experimental data in the LE (435 nm, blue) and CT (580 nm, red) spectral regions, and the superimposed curves are multiexponential fits to these data. The inset graph is an expanded view of the early time data using a linear vertical scale and showing the instrumental response function "IRF". The upper panels are the weighted residuals of double and triple exponential fits to the LE decay and a double exponential fit of the CT decay. In the case of the CT fit, the rise time was fixed to the decay time of the LE emission. Parameters of these three fits are provide in the inset table.

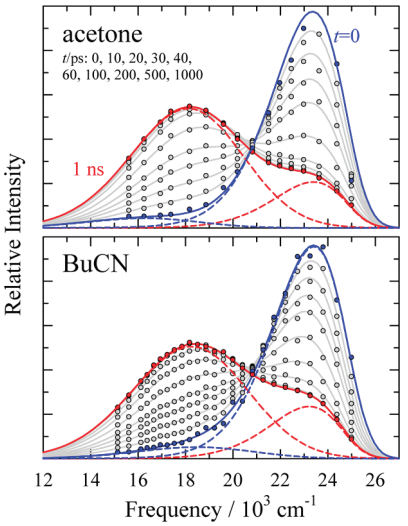

Figure 7. Area normalized time-resolved emission spectra of CVL in acetone and *n*-butyronitrile. The points are spectral data reconstructed from unconstrained fits of emission transients at each wavelength. The solid curves are fits of these reconstructed spectra data using the same procedure described for steady-state emission. The dashed curves show the component LE and CT spectra at t = 0 and 1 ns.

that this intermediate component represents impurity fluorescence, which we have not been able to eliminate completely.[24] Nevertheless, it is clear that in most conventional solvents the emission kinetics of CVL conform closely to those of a two-state interconversion process. Further evidence of this simple kinetics is provided in Figure 7, where we display representative time-resolved emission spectra of CVL collected in acetone and butyronitrile. These spectra were obtained via spectral reconstruction of unconstrained fits of emission decays collected at individual wavelengths.[15] Fitting these time-resolved spectra in the same manner as the steady-state spectra (solid curves in Figure 7) shows that the LE emission decreases in intensity synchronously with the rise of the CT emission. In solvents like acetone and butyronitrile, whose solvation times are much shorter than the 25 ps instrument response time of these experiments, the area-normalized spectra exhibit approximate isoemissive points (near 21 000 cm^{-1} in Figure 6) characteristic of a two-state process.[25] This observation is consistent with the results of Schmidhammer et al.,[12] who reported clear isosbestic points in the transient absorption of CVL in two solvents.[26] Figure 7 also shows decompositions of the t = 0 and late-time spectra into LE and CT components (dashed curves). Note that a small (~10%) CT component is apparently present at time zero. This prompt CT emission is most likely an artifact related to fitting individual decays without constraints. Fitting rise components having time constants near the instrument response time, as is the case here, is highly uncertain because rises times, amplitudes, and time shifts are all strongly correlated. When the rise times in the CT region are fixed to equal those in the better-defined decays in the LE region (as in Figure 6), no CT component is observed at time zero.

On the basis of the observations just mentioned, we interpret the time-resolved data in terms of the two-state kinetic model

Scheme 1

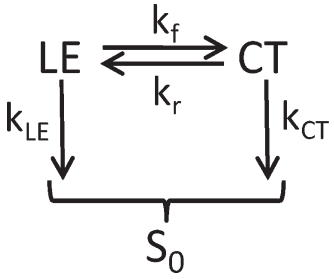

shown in Scheme 1, assuming no direct excitation of the CT state. (The present analysis is very similar to that described in ref 14, and more details can be found there.[27]) In the limit of rapid excited-state equilibrium (k_f, $k_r \gg k_{LE}$, k_{CT}) relevant here, the populations are expected to follow the relations

$$[\mathrm{LE}(t)]/[\mathrm{LE}]_0 \cong \frac{1}{k_f + k_r}\left(k_r e^{-k_{dec}t} + k_f e^{-\kappa_{rxn}t}\right) \quad (3)$$

$$[\mathrm{CT}(t)]/[\mathrm{LE}]_0 \cong \frac{k_f}{k_f + k_r}\left(e^{-k_{dec}t} - e^{-\kappa_{rxn}t}\right) \quad (4)$$

with

$$\kappa_{rxn} = k_f + k_r \quad (5)$$

and

$$k_{dec} = \frac{k_{LE}k_r + k_{CT}k_f}{k_f + k_r} \quad (6)$$

Table 3 lists parameters based on biexponential fits of time-resolved emission data of the sort shown in Figure 6 and interpreted within the context of the above model. In addition to the time constants $\tau_{rxn} = \kappa_{rxn}^{-1}$ and $\tau_{dec} = k_{dec}^{-1}$, also listed are

Table 3. Characteristics of Time-Resolved Decays and Reaction Quantities (25 °C)[a]

no.	solvent[b]	$d_c(\varepsilon)$	η/cP	$<\tau_{solv}>$/ps	a_{fast}	τ_{rxn}/ps	τ_{dec}/ns	$\ln(a_{fast}/a_{slow})$	$\ln(\nu_{LE}^3\varphi_{CT})/(\nu_{CT}^3\varphi_{LE})$	Δ_rG /kJ mol^{-1}	k_f/ns^{-1}
7	butyl acetate	0.44					18		−0.6	−0.7 ± 0.8	
8	ethyl acetate	0.48					15		−0.5	−1.0 ± 1.0	
9	methyl acetate	0.49	0.36	0.85	0.54	36	10	0.2	−0.2	−1.4 ± 0.5	18 ± 4
10	1-chlorobutane	0.51					11		−1.4	1.3 ± 1.2	
11	tetrahydrofuran	0.51					4.5		−0.5	−0.8 ± 0.9	
12	dichloromethane	0.53	0.41	0.56	0.30	70	18		1.0	−4.5 ± 0.4	12 ± 2
13	acetone	0.60	0.30	0.58	0.92	22	3.6	2.5	2.1	−6.8 ± 0.5	42 ± 10
14	butyronitrile	0.62	0.55	0.75[c]	0.92	25	4.6	2.5	2.2	−6.7 ± 0.5	37 ± 6
15	acetonitrile	0.63	0.34	0.26	0.98	8	1.2	3.9	3.4	−9.8 ± 0.9	120 ± 30
16	*N*,*N*-dimethylformamide	0.63	0.80	0.91	0.97	23	1.4	3.7	2.9	−9.2 ± 1.3	43 ± 5
17	dimethylsulfoxide	0.64	1.99	2.0	0.98	29	0.71	4.2	2.6	−10.0 ± 0.5	34 ± 3
18	propylene carbonate	0.65	2.53	2.0	0.99	30	0.6	4.5	2.3	−9.3 ± 0.5	33 ± 3
21	3:1 MeOAc + acetone	0.52	0.35	0.78	0.83	41	6.4	1.7	0.7	−3.9 ± 0.8	20 ± 6
22	2:1 MeOAc + acetone	0.53	0.34	0.76	0.83	40	5.5	1.6	0.9	−4.2 ± 0.5	21 ± 3
23	1:1 MeOAc + acetone	0.55	0.33	0.72	0.87	37	4.6	2.0	1.3	−5.2 ± 0.4	24 ± 5
24	1:2 MeOAc + acetone	0.57	0.32	0.67	0.91	27	3.5	2.4	1.6	−6.0 ± 0.4	34 ± 5
25	1:3 MeOAc + acetone	0.58	0.32	0.65	0.92	27	3.1	2.5	1.7	−6.3 ± 0.4	35 ± 5
31	1:4 PC + ACN	0.63	0.45	0.37	0.97	13	0.93	4.0	3.0	−9.8 ± 0.7	78 ± 12
32	2:3 PC + ACN	0.64	0.62	0.52	0.98	15	0.83	4.2	3.5	−10.6 ±	66 ± 9
33	3:2 PC + ACN	0.64	0.89	0.78	0.98	18	0.77	4.2	3.0	−10.2 ± 0.7	56 ± 6
34	4:1 PC + ACN	0.64	1.40	1.25	0.98	22 ± 2	0.76	4.4	2.8	−9.8 ± 0.9	45 ± 5

[a] η is the solvent viscosity and $<\tau_{solv}>$ is the integral solvation time of the C153 probe. In pure solvents, these data are taken from refs 23 and 31, respectively. In the PC + ACN mixtures, these values are from ref 32 and from volume-based interpolation between pure solvent values in the case of MeOAC + acetone mixtures. a_{fast} is the amplitude of the fast decay component of the LE emission, $\tau_{rxn} = \kappa_{rxn}^{-1}$ is the fast time constant associated with reaction, and $\tau_{dec} = k_{dec}^{-1}$ is the slow time constant associated with S_1 decay. The quantity $\ln(a_{fast}/a_{slow})$ provides an estimate of the equilibrium constant ($\ln K_{eq}$) for the LE ↔ CT reaction from time-resolved measurements, and $\ln(\nu_{LE}^3\varphi_{CT}/\nu_{CT}^3\varphi_{LE})$ is the related quantity from the steady-state spectra. Δ_rG is the free energy change in the reaction determined as a weighted average of these two estimates, and k_f is the forward (LE → CT) rate constant. [b] MeOAc = methylacetate, ACN = acetonitrile, and *n*:*m* indicates mixture compositions by volume. [c] Value of $<\tau_{solv}>$ for butyronitrile is estimated.

values of the normalized amplitudes a_{fast} of the fast component of emission measured on the blue side of the LE band where CT emission is negligible. Some comparisons of the time constants observed are available from the work of Karpiuk and coworkers.[3,12] For the six solvents in which there is overlap, the values of τ_{dec} reported here average 15% smaller than those previously reported.[3] This systematic difference can be reasonably ascribed to either a difference in deoxygenation techniques or to the different time resolutions available (~1 ns in the case of ref 3) More important is a comparison of the fast time constants τ_{rxn} with the transient absorption data of Schmidhammer et al.[12] Using an instrument with 300 fs resolution, these authors reported LE and CT rise and decay times of 8.6 ± 0.4 ps in acetonitrile, 28 ± 6 ps in propylene carbonate, and 14 ± 2 ps in dimethylsulfoxide. In the case of the first two solvents, our data agree quantitatively with their results. This agreement, especially in the case of acetonitrile, supports the idea that one can measure time constants that are comparable to or even significantly smaller than the 25 ps instrument response time of the TCSPC instrument with reasonable accuracy. However, the present result in DMSO, 29 ± 3 ps, is markedly different from that of Schmidhammer et al. The reason for this difference is unknown.

Before discussing the kinetic parameters in Table 3 in more detail, we first use these data to estimate the equilibrium constant for the LE → CT reaction. According to eq 3 $a_{fast} = k_f/(k_f + k_r)$ so that a_{fast} is related to the equilibrium constant via

$$K_{eq} = \frac{k_f}{k_r} = \frac{a_{fast}}{1 - a_{fast}} \tag{7}$$

In the rapid-reaction limit, the ratio of band intensities or quantum yields φ in steady-state spectra are also related to the equilibrium constant as follows

$$\frac{\varphi_{CT}}{\varphi_{LE}} = \frac{k_{rad}^{CT}}{k_{rad}^{LE}}\frac{k_f}{k_r} = \frac{k_{rad}^{CT}}{k_{rad}^{LE}}K_{eq} \tag{8}$$

Making the assumption that ratios of radiative rates in different solvents depend only on emission frequencies due to the relation $k_{rad} \propto \nu_{em}^3$, equilibrium constants can be estimated from steady-state data to within a constant factor *C* via

$$K_{eq} = C\frac{\nu_{LE}^3\varphi_{CT}}{\nu_{CT}^3\varphi_{LE}} \tag{9}$$

Both measures of K_{eq} are provided in logarithmic form in Table 3. A weighted average of the differences between the time-resolved and steady-state estimates yields $C = 2.4 \pm 0.3$. Using this value of *C*, we compare the two estimates of K_{eq} in Figure 8a. As shown here, there is reasonable agreement between the steady-state and time-resolved estimates. Reaction free energies, Δ_rG, obtained from a combination of these K_{eq} values via $\Delta_rG = -RT\ln K_{eq}$, are also summarized in Table 3. We note that the values determined in highly polar solvents are somewhat larger than the values of −3 to −4 kJ/mol estimated by Schmidhammer et al.[12] on the basis of less direct information (but much smaller than the previous estimate of −57 kJ/mol[3]). The present values of Δ_rG are plotted versus the dielectric reaction field factor $d_c(\varepsilon)$ in Figure 8b. With a few exceptions such as dichloromethane (no. 10), the correlation between Δ_rG and $d_c(\varepsilon)$ is good. Using the same model

dx.doi.org/10.1021/jp106240x | J. Phys. Chem. A 2011, 115, 3746–3754

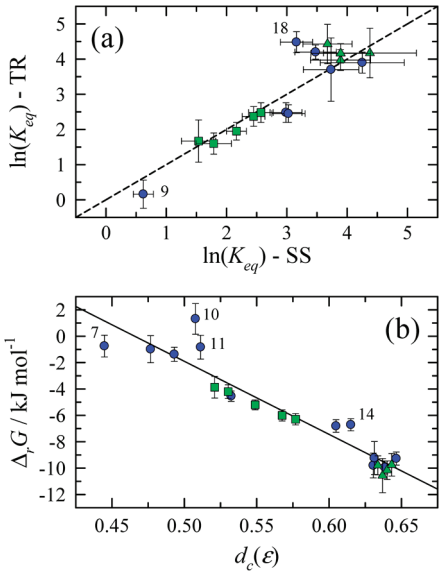

Figure 8. Equilibrium constant and free energy change of the LE → CT reaction. (a) Comparison of equilibrium constants determined from relative amplitudes of the LE decay ("TR") and from relative intensities of steady-state CT and LE emission ("SS"). (b) Estimates of reaction free energies determined from weighted averages of the ln K_{eq} data versus dielectric reaction field factor $d_c(\varepsilon)$. The line drawn in this panel is the regression $\Delta_r G$/kJ mol^{-1} = 25.8 − 55.4$d_c(\varepsilon)$ (r^2 = 0.90). The green squares are data from mixtures of acetone + methyl acetate and green triangles from propylene carbonate + acetonitrile mixtures. Numbers indicate specific solvents, as listed in Table 3.

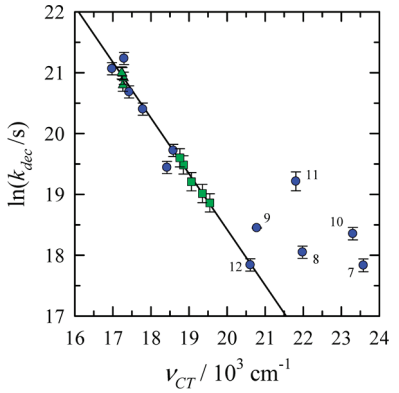

Figure 9. Decay rate constants k_{dec} associated with the slower emission decay component plotted versus CT frequency. The blue points are data in pure solvents and the green squares and triangles are data in mixtures of acetone + methyl acetate and propylene carbonate + acetonitrile, respectively. Numbers indicate specific solvents as listed in Table 3.

employed for solvatochromic analysis, the slope in such a plot is expected to be given by

$$\frac{d(\Delta_r G)}{d(d_c)} = -\left(\frac{\mu_{CT}^2}{a_{CT}^3} - \frac{\mu_{LE}^2}{a_{LE}^3}\right) \quad (10)$$

The observed value, −55 kJ/mol, is consistent with the estimates of the LE and CT dipole moments determined from analysis of frequency shifts. Using Karpiuk's[3] values for cavity radii once again, a_{LE} = 3.6 Å and a_{CT} = 5.8 Å, and the estimate μ_{CT} = 24 D, the observed slope implies μ_{LE} = 9.7 D, which is in the middle of the range 9−12 D suggested by the solvatochromic analysis.

We now consider the solvent dependence of the kinetic quantities in Table 3. In Figure 9, we plot the average decay rate, $k_{dec} = 1/\tau_{dec}$, as a function of the peak CT emission frequency. In solvents more polar than acetone, there is a good correlation between ν_{CT} and the logarithm of k_{dec}. In these solvents, for which $K_{eq} > 4$, eq 6 indicates that k_{dec} should be approximately equal to k_{CT}, the rate constant for CT-state decay. We note that the values of $k_{dec} \cong k_{CT}$ measured here as well as their dependence upon ν_{CT} are quite similar to what was reported for the CT-state analogue malachite green lactone.[10] In the latter case, Karpiuk attributed the emission decay rate to the internal conversion CT → S_0 and the exponential relationship between k_{dec} and ν_{CT} to a manifestation of the energy gap law.[10] It is reasonable to adopt this same interpretation in the case of CVL, at least in sufficiently polar solvents.

Rate constants for the forward reaction (LE → CT) calculated from κ_{rxn} and K_{eq} via

$$k_f = \frac{\tau_{rxn}^{-1}}{1 + K_{eq}^{-1}} \quad (11)$$

are listed in the final column of Table 3. These rate constants are plotted in Figure 10 as functions of both viscosity (η/T) and average solvation time $\langle\tau_{solv}\rangle$. In addition to the data listed in Table 3, we have included data from temperature-dependent measurements in propylene carbonate and butyronitrile (small open symbols and regression lines). Motivating the choice of independent variables here is the expectation that the LE → CT reaction is significantly influenced by dynamical solvent effects.[12] If the reaction involves some large amplitude motion of the solute, then one might expect the friction on this motion to be proportional to (η/T), as predicted by hydrodynamics. If, alternatively, the primary nuclear coordinates comprising the reaction coordinate are solvent coordinates, then an inverse proportionality to solvation times might be expected. The data in Figure 10 show that the reaction rates are correlated to both η/T and $\langle\tau_{solv}\rangle$. As suggested by the color coding in this figure, which groups solvents according to polarity, reaction energetics is also an important determinant of the rates. The most polar solvents, those with driving forces $-\Delta_r G > 9$ kJ/mol (red points), approximately follow a single correlation with either measure of solvent friction. Points with successively smaller driving force (6−9 kJ/mol = green and <6 kJ/mol = blue) show slower reactions for a given value of η/T or $\langle\tau_{solv}\rangle$. Such variations can be readily understood as reflecting proportionate lowering of the barrier to reaction with increasing driving force $-\Delta_r G$. Such a dependence is expected based on either Marcus theory in the normal regime or simple Brønsted arguments. In prior work on aminobenzonitriles,[14] we were able to approximately disentangle this equilibrium energetic effect from the solvent dynamical effect. Although the present data do not permit such an analysis, it seems reasonable to assume that the same situation pertains here. In any case, the additional dependence on solvent polarity does not obscure the connection to solvent friction, at least in the highly polar solvents.

Whether the frictional effect is the result of solute (η/T) or solvent $(\langle\tau_{solv}\rangle)$ motions cannot be decided solely on the basis of the comparisons in Figure 10. In the solvents suitable for CVL experiments (i.e., excluding the normal alcohols), viscosity and solvation time are approximately proportional to one another, and thus the correlations of either variable with τ_{rxn} are of comparable quality. However, electronic structure calculations[19] indicate that steric hindrance prevents any large-amplitude

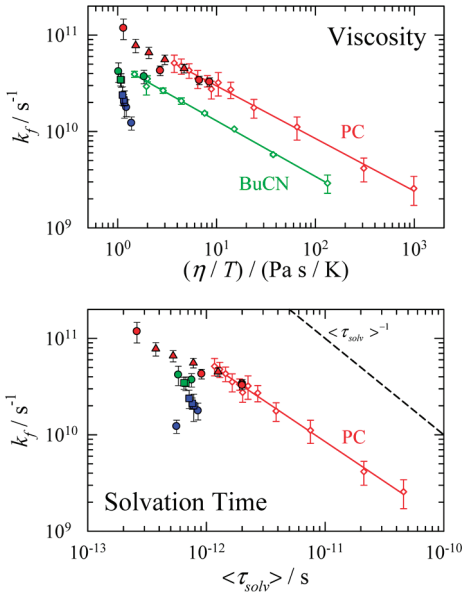

Figure 10. Forward reaction rate constants k_f plotted versus viscosity (η/T) and solvation time $<\tau_{solv}>$. Larger symbols are the data listed in Table 3. The colors indicate relative polarity: blue = least polar ($n < 12$), green = intermediate polarity (nos. 13,14), and red = most polar (n = 15−18) solvents. The small open symbols and regression lines are temperature dependent data in butyronitrile (BuCN; 170−310 K) and propylene carbonate (PC; 210−340 K). Viscosity data for these points are from parameterizations of literature data,[33] and the solvation times in propylene carbonate are from measurements of Berg and coworkers using the *s*-tetrazine probe.[34] The slopes of the temperature-dependent data indicate relations $k_f \propto (\eta/T)^{-p}$ with powers $p = 0.54$ (PC) and 0.58 (BuCN) and $k_f \propto <\tau_{solv}>^{-p}$ with $p = 0.83$ (PC).

motion of the dimethylaniline donor groups, which are the most likely candidates for solute motions that would couple to solvent viscosity. For this reason, we favor interpreting the LE → CT reaction as an adiabatic electron transfer process whose reaction coordinate involves primarily solvent polarization modes and is therefore controlled by solvation dynamics. In support of this interpretation, we note that in ionic liquid solvents we[8] and Samanta and coworkers[6] observe near equality between estimates of τ_{rxn} and $<\tau_{solv}>$. In contrast, in the highly polar conventional solvents studied here, τ_{rxn} is about 10 times larger than $<\tau_{solv}>$, which implies a small but significant barrier to reaction (~1 to 2 k_BT) in these solvents.

4. SUMMARY AND CONCLUSIONS

In the present work, we have surveyed the steady-state and time-resolved emission of CVL in a variety of aprotic solvents. Analysis of the solvatochromism of the LE and CT bands measured here using a different dielectric continuum model leads to essentially the same results previously reported by Karpiuk.[3] The dipole moments of the LE and CT states are estimated to be 9−12 and ~24 D, respectively. Because these values depend strongly on the choice of cavity radii, they should only be considered to provide a rough indication of the relative polarities of the two excited states. Nevertheless, these dipole moments support a description of the LE → CT reaction as involving a full electron transfer between the aminobenzene and aminophthalide groups.

Analysis of the relative intensities of the LE and CT emission bands, together with information from time-resolved data, enables determination of free energy changes Δ_rG associated with the LE → CT reaction. These free energies are reasonably correlated to solvent dielectric properties using the same dielectric continuum model used to analyze the solvatochromic shifts. The solvent dependence is such that Δ_rG ranges between +14 kJ/mol in *n*-hexane to −10 kJ/mol in propylene carbonate, with $\Delta_rG = 0$ occurring for dielectric constants between 5 and 6.

The emission kinetics of CVL largely conform to expectations for a two-state reaction between the LE and CT states. In moderately to strongly polar solvents near room temperature, emission decays are close to biexponential in form, consisting of a dominant component with a time constant of 8−40 ps related to LE ↔ CT equilibration, and a minor component with a nanosecond lifetime due to decay of the equilibrated excited-state population. In high polarity solvents the lifetime is determined primarily by the nonradiative decay of the CT state to S_0, which is exponentially related to the CT−S_0 energy gap, similar to what was previously observed in malachite green lactone.[10] The rates of the LE → CT reaction appear to be sensitive to both solvent polarity and to solvent friction. At least within the highest polarity solvents examined here there is a good correlation of the reaction rates (or τ_{rxn}) with both solvent viscosity and solvation times. The simplest description of the reaction consistent with these observations is that of an adiabatic electron transfer on a 1-D reaction coordinate comprised primarily of solvent polarization modes and having a modest barrier to reaction. More complicated scenarios involving fast equilibration with vibrational modes of the solute, as proposed by Schmidhammer et al.,[12] are equally consistent with the data. Quantitative modeling of the reaction rates and additional data with higher time resolution are needed to determine which perspective is more correct.

AUTHOR INFORMATION

Corresponding Author
*E-mail: maroncelli@psu.edu.

ACKNOWLEDGMENT

This work was funded by the Division of Chemical Sciences, Geosciences, and Biosciences, Office of Basic Energy Sciences of the U.S. Department of Energy through grant DE-FG02-89ER14020. We also thank Lasse Jensen for performing DFT calculations of CVL.

REFERENCES

(1) Kaneko, Y.; Neckers, D. C. *J. Phys. Chem. A* **1998**, *102*, 5356.
(2) Karpiuk, J. *Ann. Polish Chem. Soc.* **2001**, 271.
(3) Karpiuk, J. *J. Phys. Chem. A* **2004**, *108*, 11183.
(4) Jin, H.; Li, X.; Maroncelli, M. *J. Phys. Chem. B* **2007**, *111*, 13473.
(5) Annapureddy, H. V. R.; Margulis, C. J. *J. Phys. Chem. B* **2009**, *113*, 12005.
(6) Santhosh, K.; Samanta, A. *J. Phys. Chem. B* **2010**, *114*, 9195.
(7) Jin, H.; Li, X.; Maroncelli, M. *J. Phys. Chem. B* **2010**, *114*, 11370.
(8) Li, X.; Maroncelli, M. *J. Phys. Chem. B*, manuscript in preparation.
(9) Allen, N. S.; Hughes, N.; Mahon, P. *J. Photochem.* **1987**, *37*, 379.
(10) Karpiuk, J. *Phys. Chem. Chem. Phys.* **2003**, *5*, 1078.
(11) Karpiuk, J. *Phys. Chem. Chem. Phys.* **2005**, *7*, 4070.
(12) Schmidhammer, U.; Megerle, U.; Lochbrunner, S.; Riedle, E.; Karpiuk, J. *J. Phys. Chem. A* **2008**, *112*, 8487.

(13) Karpiuk, J.; Karolak, E.; Nowacki, J. *Pol. J. Chem.* **2008**, *82*, 865.
(14) Dahl, K.; Biswas, R.; Ito, N.; Maroncelli, M. *J. Phys. Chem. B* **2005**, *109*, 1563.
(15) Maroncelli, M.; Fleming, G. R. *J. Chem. Phys.* **1987**, *86*, 6221.
(16) As a check on the present results, we recorded several spectra using a different fluorimeter from the one used to collect the results reported here and obtained nearly identical spectra.
(17) Fee, R. S.; Milsom, J. A.; Maroncelli, M. *J. Phys. Chem.* **1991**, *95*, 5170.
(18) Arzhantsev, S.; Zachariasse, K.; Maroncelli, M. *J. Phys. Chem. A* **2006**, *110*, 3454.
(19) Jensen, L. Unpublished calculations, 2010.
(20) Stevens, B.; Ban, M. I. *Trans. Faraday Soc.* **1964**, *60*, 1515.
(21) Zachariasse, K. A. *Trends Photochem. Photobiol.* **1994**, *3*, 211.
(22) Grabowski, Z. R.; Rotkiewicz, K.; Rettig, W. *Chem. Rev.* **2003**, *103*, 3899.
(23) Marcus, Y. *The Properties of Solvents*; Wiley: New York, 1998.
(24) Because the emission quantum yields of CVL in polar solvents are in the range 0.004 to 0.023, solvent impurities and contributions of Raman scattering interfere with decay measurements more than in typical fluorescence probes. In some cases, we subtracted transients obtained from solvent blanks before fitting the emission decays, which tends to reduce but not eliminate the relative magnitude of the intermediate component.
(25) Koti, A. S. R.; Krishna, M. M. G.; Periasamy, N. *J. Phys. Chem. A* **2001**, *105*, 1767.
(26) In solvents having slow solvation responses such as ionic liquids, the LE band undergoes a dynamic Stokes shift, which typically spoils this simple behavior.[8] Interestingly, in one ionic liquid, Santhosh and Samanta[6] report a clear isoemissive point despite a significant dynamic Stokes shift of the LE band.
(27) Equation 3.7 of ref 14 is incorrect; Equation 6 is the corrected version.
(28) Barthel, J.; Neueder, R.; Roch, H. *J. Chem. Eng. Data* **2000**, *45*, 1007.
(29) Barthel, J.; Utz, M.; Gross, K.; Gores, H. J. *J. Solution Chem.* **1995**, *24*, 1109.
(30) Bondeau, A.; Huck, J. *J. Phys. (Les Ulis, Fr.)* **1985**, *46*, 1717.
(31) Horng, M. L.; Gardecki, J. A.; Papazyan, A.; Maroncelli, M. *J. Phys. Chem.* **1995**, *99*, 17311.
(32) Gardecki, J. A.; Maroncelli, M. *Chem. Phys. Lett.* **1999**, *301*, 571.
(33) Propylene carbonate viscosity data are from refs 28−30, which fit to the relation $\ln(\eta/\mathrm{cP}) = -2.181 + 456.2/(T/\mathrm{K} - 149.03)$ valid between 205−400 K. Butyronitrile viscosities are from ESDU Physical Data, Chemical Engineering Series (http://www.esdu.com/) which fit to $\ln(\eta/\mathrm{cP}) = -3.405 + 644.3/(T/\mathrm{K} - 68.33)$ over the temperature range 175−375 K.
(34) Ma, J.; Bout, D. V.; Berg, M. *J. Chem. Phys.* **1995**, *103*, 9146.